

Locating Laser Sensors for Projector Touch Screens using Trigonometric Methods

Sang-Young Cho

Department of Computer Engineering

Hankuk University of Foreign Studies

81 Oedae-ro Mohyen-eup Cheoin-gu Yongin-si Gyeonggi-do 17035

KOREA

sycho@hufs.ac.kr

Abstract: - An interactive whiteboard can either be a standalone computer with touchscreen or a large functioning touchpad for computer display. Interactive whiteboard systems with laser optic modules can overcome the high cost, low resolution, and low scalability of large touchscreens. Recently, a trigonometric method to find the positions of laser optic modules has been suggested to install the whiteboard system with the laser optic module. The method calculates the geometrical positions of laser optic modules using the sensed angle values of the three touched points on a whiteboard display. Three patterns of touched points are used and trigonometric expressions are derived for each pattern. This paper derived trigonometric expressions that generalize the expressions for three different patterns. Using the derived expressions, we showed that the expression set for each pattern is a special case of the generalized trigonometric expression set.

Key-Words: - Interactive whiteboard, Touchscreen, Calibration, Trigonometric, Locating problem.

1 Introduction

An interactive whiteboard (IWB) can either be a standalone computer with touchscreen or a large functioning touchpad for computer display. Usually, a device driver is installed on the attached computer so that the IWB can act as a human input device. In cases of an IWB that uses a projector, the computer's video output is connected to a digital projector so that images can be projected on the IWB screen. Users can then point and control the display objects on the whiteboard by using their fingers or stylus pens as a mouse directly on the screen. They are used in various settings such as classrooms for education, seminar rooms for corporate members, training rooms for coaching, studios for broadcasting, and others [1].

The way to implement an IWB is heavily dependent on touchscreen technologies such as resistive, surface acoustic wave, capacitive, infrared grid, infrared acrylic projection, optical imaging, and dispersive signal technology [2]. A touchscreen technology determines the quality and property of the implemented IWB. A touchscreen is an input and output device usually layered on the top of an electronic visual display of a computer system. A user can give input or control the computing system through simple or multi-touch gestures by touching the screen with a special stylus or one or more fingers [3].

Resistive technology is the first generation of touchscreens [4]. It uses two transparent electrically resistive layers. This technology suffers from poor durability and optical quality, and lack of multi-touch. Capacitive-based touch panels arrange electrodes as rows and columns. The electrodes are separated by an insulating material [5]. It has disadvantage of high manufacturing cost when the size of touchscreen becomes large. In surface acoustic wave schemes, the touch position is detected by acoustic waves [6]. It requires heavy force for touch and bezel to cover reflectors. The infrared grid technology uses an infrared grid pattern [7]. The technology is not adequate for interactive touchscreen applications due to low resolution, slow speed, and the size constraint of touch objects.

For camera-based optical technology, backlights of IR LEDs are provided in the corners of the touchscreen with a retroreflector around the periphery of the screen [8]. When a finger touches the display, it interrupts the light and a shadow is seen by the cameras. Then the location of touch can be calculated with image processing. It suffers from low resolution but has advantage of lower cost for larger touch screen. There are several researches for human-machine interaction beyond 2-D touch interface [9, 10].

Even though a touchscreen computer can be used for IWBs, touchscreen display technique suffers

from high-cost and implementation difficulty for more than 100-inch displays [11]. Therefore, cheap and scalable touchscreen methods have been used for IWB implementation. [12] introduced an IWB system that uses a laser optic module to overcome the high cost and difficulties in implementation of large touch size. The system can locate touches more accurately by using laser emitter instead of LED. The system based on laser optic modules requires triangulation calculations for installation. The method calculates the geometrical positions of laser optic modules using the sensed angle values of the three touched points on a whiteboard display. Three patterns of touched points are used and trigonometric expressions are derived for each pattern. In this paper, we generalize the trigonometric methods developed in [12]. Using the derived expressions, we show that the expression set for each pattern is a special case of the generalized trigonometric expression set.

This paper organized as follows. In Section 2, we present the operation principals of the IWB system based on laser optic modules, and formulates the problems. We derives generalized trigonometric expressions for locating laser optic modules and shows that the expressions are specialized to the three pattern cases in Section 3. The paper concludes with Section 4.

2 Problem Formulation

Fig. 1 shows an ideal installation of the display of a whiteboard system with laser optic modules.

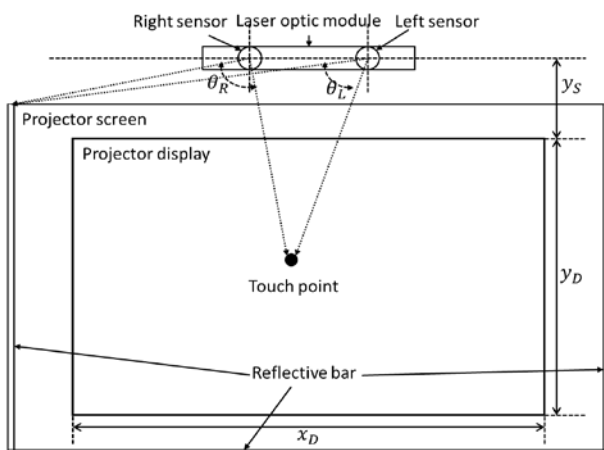


Fig. 1 The operational view of a laser optic module whiteboard.

The laser optic module contains two right and left laser sensors. Each laser sensor has a red laser emitter, a light detector, and a 7200-rpm motor that rotates 45-degree prism counterclockwise. Three

reflective bars are installed right, down, and left sides of the projector screen. The light beam from each laser sensor rotates along the reflective bar and non-reflection path. The reflected light from reflective bars can reach the light detector if there is no touch on the projector screen. The light detector generates high signal if it detects light. The detector generates low signal when the beam scans the non-reflection path or when a touching object absorbs and scatters the beam. Using the generated signals of the light detectors, we obtain angles θ_R and θ_L . A projector that projects a computer display output forms a projector display on the projector screen. We can know all the geometrical values of the projector screen, the projector display, and the laser optic module in an ideal installation case. However, every installations have errors due to incorrect installation of the screen, projector, and laser optic module. Errors also occur due to optical errors in the laser optic module and the projector. This installation error incurs an incorrect calculation of touch points.

The severer problem is the size and aspect ratio of the projector display shot by the actual projector. By the installation and optical errors of the projector, the IWB system may suffer from an image distortion. The larger the display plane, the more error it produces. The size of screen image shot by the actual projector cannot be determined in advance, and after the installation, it is necessary to adjust the shape of the projected image.

To resolve the problems of installation and projection errors, [12] addressed the methods that calculate the geometrical positions of laser optic modules using the sensed angle values of the three touched points on a whiteboard display. Three patterns of touched points are used and trigonometric expressions are derived for each pattern. The patterns are for 1) Geometric Position of Laser Sensors, 2) Finding x-y Distortion Ratio, and 3) Distortion Check at Corners of Projector Display. We derive trigonometric expressions that generalize the expressions for three different patterns. In order to determine each geometrical value of an IWB system on the 2-D plane, a metric unit and a reference point is required for specifying the location of each point. The correct invariant information of the system is the resolution of the projector display because it is set by the computer that originates the display.

For the case of "Geometric Position of Laser Sensors", [12] used three touch points located on a line that is parallel to the laser optic module as shown in Fig. 2.

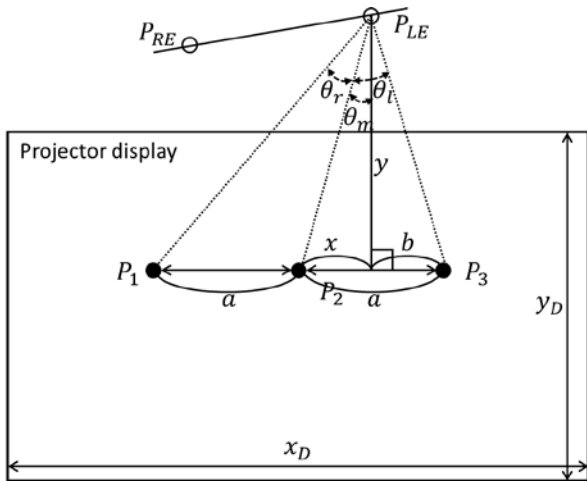


Fig. 2 Geometrical values for laser sensor locations.

The three points (P_1, P_2, P_3) are displayed with fixed positions. The distance between P_1 and P_2 be the same to the distance between P_2 and P_3 with a pixel size units. By touching each point, the measured angle of the point can be obtained from the light detector signal. Then θ_r can be obtained by subtracting the measured angle of P_1 from the measured angle of P_2 . Similarly, θ_l is obtained with the measured angles of P_2 and P_3 . The position of the left sensor is expressed with the following expressions

$$\tan \theta_m = \frac{\tan \theta_l - \tan \theta_r}{2 \tan \theta_r \tan \theta_l} \quad (1)$$

$$y = \frac{a}{\tan(\theta_r + \theta_m) - \tan \theta_m}, \quad x = y \tan \theta_m \quad (2)$$

For the case of “Finding x-y Distortion Ratio”, [12] used three touch points located on a line that is perpendicular to the laser optic module as shown in Fig. 3.

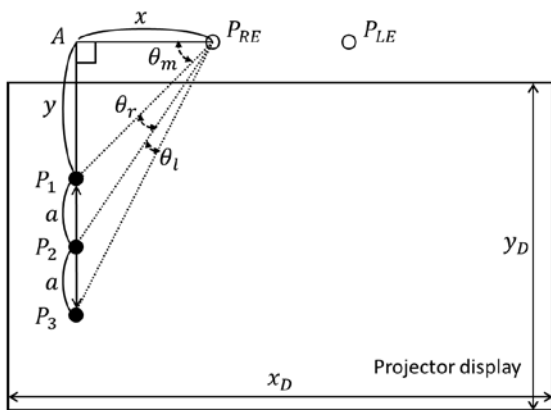


Fig. 3 Finding x-y distortion using three vertical points.

The following expressions are used to find x-y distortion.

$$\tan \theta_m = \frac{2 \tan \theta_r - \tan(\theta_r + \theta_l)}{\tan \theta_r \tan(\theta_r + \theta_l)} \quad (3)$$

$$x = \frac{a}{\tan(\theta_r + \theta_m) - \tan \theta_m}, \quad y = x \tan \theta_m \quad (4)$$

For the case of “Distortion Check at Corners of Projector Display”, [12] used three touch points located on the right down corner so as to form L shape as shown in Fig. 4.

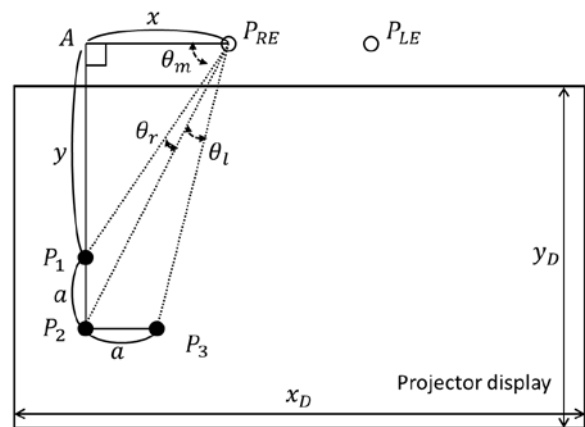


Fig. 4 Checking distortion using three points at corner areas.

The following expressions are used to check distortion of corners.

$$\tan \theta_m = \frac{\tan(\theta_r + \theta_l)}{\tan \theta_r} - \tan(\theta_r + \theta_l) - 1 \quad (5)$$

$$x = \frac{a}{\tan(\theta_r + \theta_m) - \tan \theta_m}, \quad y = x \tan \theta_m \quad (6)$$

The three touch patterns above can be generalized as shown in Fig. 5.

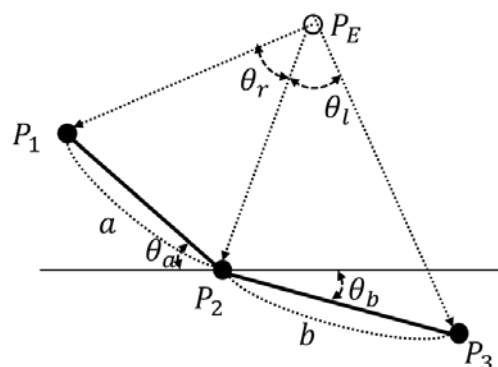


Fig. 5 A generalized view of the three touch patterns.

The first touch pattern is a special case of Fig. 5 where $\theta_a = \theta_b = 0^\circ$ and $a = b$. The second touch pattern is a special case of Fig. 5 where $\theta_a = \theta_b = 90^\circ$ and $a = b$. Finally, Fig. 4 is the case of where $\theta_a = 90^\circ$, $\theta_b = 0^\circ$, and $a = b$.

Given the three points in Fig. 5, we derive trigonometric expressions that generalize the expressions for three different patterns.

3 Problem Solution

To extract generalized trigonometric expressions for finding location of the laser sensor P_E , we assume that the origin of the coordinate plane of Fig. 5 is P_2 . Some lines and values are added on Fig. 5 to facilitate the derivation of generalized expressions as shown in Fig. 6.

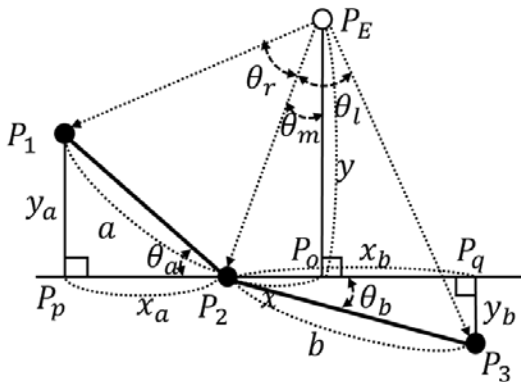


Fig. 6 Geometrical values to find the location of P_E from the origin P_2 .

Let the distance of the line (P_1, P_2) be a and the distance of (P_2, P_3) be b with a pixel size units. The angles θ_a and θ_b are known priori and the angles θ_r and θ_l are measured by P_E . We draw three perpendicular lines to the x axis from P_1 , P_E , and P_3 : (P_1, P_p) , (P_E, P_o) , and (P_3, P_q) . Let the lengths of the three lines be y_a , y , and y_b , respectively. Let the lengths of (P_2, P_p) , (P_2, P_o) , and (P_2, P_q) be x_a , x , and x_b . Then, $x_a = a \cos \theta_a$, $y_a = a \sin \theta_a$, $x_b = b \cos \theta_b$, and $y_b = b \sin \theta_b$.

Using the tangent definition, we can get the following expressions Eq. (7), Eq. (8), and Eq. (9).

$$\tan \theta_m = x/y \tag{7}$$

$$\tan(\theta_r + \theta_m) = (x + x_a)/(y - y_a) \tag{8}$$

$$\tan(\theta_l - \theta_m) = (x_b - x)/(y + y_b) \tag{9}$$

Using the tangent addition theorem, we can get Eq. (10) from Eq. (8).

$$(y - y_a)(\tan \theta_r + \tan \theta_m) = (x + x_a)(1 - \tan \theta_r \tan \theta_m) \tag{10}$$

By applying Eq. (7) to Eq. (10) and simplifying it in terms of y ,

$$y = \frac{y_a(\tan \theta_r + \tan \theta_m) + x_a(1 - \tan \theta_r \tan \theta_m)}{\tan \theta_r(1 + \tan^2 \theta_m)} \tag{11}$$

Similarly, we can get Eq. (12) and Eq. (13) from Eq. (7) and Eq. (9).

$$(y + y_b)(\tan \theta_l - \tan \theta_m) = (x_b - x)(1 + \tan \theta_l \tan \theta_m) \tag{12}$$

$$y = \frac{-y_b(\tan \theta_l - \tan \theta_m) + x_b(1 + \tan \theta_l \tan \theta_m)}{\tan \theta_l(1 + \tan^2 \theta_m)} \tag{13}$$

From Eq. (11) and Eq. (13),

$$\frac{y_a(\tan \theta_r + \tan \theta_m) + x_a(1 - \tan \theta_r \tan \theta_m)}{\tan \theta_r(1 + \tan^2 \theta_m)} = \frac{-y_b(\tan \theta_l - \tan \theta_m) + x_b(1 + \tan \theta_l \tan \theta_m)}{\tan \theta_l(1 + \tan^2 \theta_m)} \tag{14}$$

By simplifying Eq. (14) in terms of $\tan \theta_m$, Eq. (15) is obtained.

$$\tan \theta_m = \frac{\tan \theta_r \tan \theta_l (y_a + y_b) - x_b \tan \theta_r + x_a \tan \theta_l}{\tan \theta_r \tan \theta_l (x_a + x_b) + y_b \tan \theta_r - y_a \tan \theta_l} \tag{15}$$

From Eq. (7) and Eq. (8), y and x can be calculated with Eq. (16) and Eq. (17).

$$y = \frac{y_a \tan(\theta_r + \theta_m) + x_a}{\tan(\theta_r + \theta_m) - \tan \theta_m} \tag{16}$$

$$x = y \tan \theta_m \tag{17}$$

The expressions of Eq. (15), Eq. (16), and Eq. (17) are the generalized expressions for the three touch patterns to compensate the installing and projection errors. We verify the generality of the expressions by applying the specific values of each pattern to the derived expressions. We focus on Eq. (15) because the verification of Eq. (16) and Eq. (17) may be straightforward.

In case of the first touch pattern for laser sensor location, $\theta_a = \theta_b = 0^\circ$ and $a = b$. Then, $x_a = a$, $y_a = 0$, $x_b = a$, and $y_b = 0$. Eq. (18) shows Eq. (15) is induced from Eq. (15) using the specific values.

$$\tan \theta_m = \frac{-a \tan \theta_r + a \tan \theta_l}{\tan \theta_r \tan \theta_l (a + a)} = \frac{\tan \theta_l - \tan \theta_r}{2 \tan \theta_r \tan \theta_l} \tag{18}$$

In case of the second touch pattern to find x - y distortion, $\theta_a = \theta_b = 90^\circ$ and $a = b$. Then,

$x_a = 0, y_a = a, x_b = 0,$ and $y_b = a$. We apply the values to Eq. (15) and get Eq. (19).

$$\tan \theta_m = \frac{2 \tan \theta_r \tan \theta_l}{\tan \theta_r - \tan \theta_l} \quad (19)$$

The θ_m of Eq. (3) notates a different angle to the θ_m of Eq. (19). Eq. (19) becomes Eq. (20) if we rewrite Eq. (19) using the angle θ_m of Eq. (3).

$$\tan(90^\circ - \theta_m - \theta_r) = \frac{2 \tan \theta_r \tan \theta_l}{\tan \theta_r - \tan \theta_l} \quad (20)$$

By using $\tan(90^\circ - \theta) = \cot \theta$ and applying the tangent addition theorem,

$$\frac{1 - \tan \theta_m \tan \theta_r}{\tan \theta_m + \tan \theta_r} = \frac{2 \tan \theta_r \tan \theta_l}{\tan \theta_r - \tan \theta_l} \quad (21)$$

By simplifying Eq. (21) in terms of $\tan \theta_m$,

$$\tan \theta_m = \frac{2 \tan \theta_r (1 - \tan \theta_r \tan \theta_l) - (\tan \theta_r + \tan \theta_l)}{\tan \theta_r (\tan \theta_r + \tan \theta_l)} = \frac{2}{\tan(\theta_r + \theta_l)} - \frac{1}{\tan \theta_r} = \frac{2 \tan \theta_r - \tan(\theta_r + \theta_l)}{\tan \theta_r \tan(\theta_r + \theta_l)} \quad (22)$$

In case of the third touch pattern to check the distortions of display corners, $\theta_a = 90^\circ, \theta_b = 0^\circ,$ and $a = b$. Then, $x_a = 0, y_a = a, x_b = a,$ and $y_b = 0$. We apply the values to Eq. (15) and get Eq. (23).

$$\tan \theta_m = \frac{\tan \theta_r \tan \theta_l - \tan \theta_r}{\tan \theta_r \tan \theta_l - \tan \theta_l} \quad (23)$$

The θ_m of Eq. (5) notates a different angle to the θ_m of Eq. (23). Eq. (23) becomes Eq. (24) if we rewrite Eq. (23) using the angle θ_m of Eq. (5).

$$\tan(90^\circ - \theta_m - \theta_r) = \frac{\tan \theta_r \tan \theta_l - \tan \theta_r}{\tan \theta_r \tan \theta_l - \tan \theta_l} \quad (24)$$

By using $\tan(90^\circ - \theta) = \cot \theta$ and applying the tangent addition theorem,

$$\frac{1 - \tan \theta_m \tan \theta_r}{\tan \theta_m + \tan \theta_r} = \frac{\tan \theta_r \tan \theta_l - \tan \theta_r}{\tan \theta_r \tan \theta_l - \tan \theta_l} \quad (25)$$

By simplifying Eq. (25) in terms of $\tan \theta_m$,

$$\tan \theta_m = \frac{\tan \theta_l + \tan \theta_r (\tan \theta_r + \tan \theta_l) + \tan^2 \theta_r \tan \theta_l}{\tan \theta_r (1 - \tan \theta_r \tan \theta_l)} = \frac{\tan \theta_l + \tan \theta_r - \tan \theta_r + \tan^2 \theta_r \tan \theta_l}{\tan \theta_r (1 - \tan \theta_r \tan \theta_l)} + \tan(\theta_r + \theta_l) = \frac{\tan(\theta_r + \theta_l)}{\tan \theta_r} + \tan(\theta_r + \theta_l) - 1 \quad (26)$$

With Eq. (18), Eq. (22), and Eq. (26), we showed that the expressions of Eq. (15), Eq. (16), and Eq. (17) are the generalized expressions for the three touch patterns to compensate the installing and projection errors.

4 Conclusion

Interactive whiteboards using laser optical module have the advantage that only two laser sensors are used regardless of the size of the screen and the position of the touch point can be accurately obtained even when the screen is enlarged. Large interactive whiteboards are usually assembled using projectors. However, it is not easy to install the projector and touch apparatus accurately due to their large screen size and inherent mechanical and optical errors. Also, the characteristics of components may change by times and the initial settings may be not adequate to the changed states.

In this paper, we derived trigonometric expressions that generalize the expressions for three different patterns of previous work. Using the derived expressions, we showed that the expression set for each pattern is a special case of the generalized trigonometric expression set. The derived expression can be used to extract the information needed for management of interactive whiteboards through minimum computation based on the angle data measured by the optical module.

Acknowledgements

This work was supported by Hankuk University of Foreign Studies Research Fund of 2019.

References:

- [1] J. Dostal, Reflections on the Use of Interactive Whiteboards in Instruction in International Context, *The New Educational Review*, Vol. 25, No. 3, 2011, pp. 205-220.
- [2] G. Walker, A Review of Technologies for Sensing Contact Location on the Surface of a Display, *Journal of the Society for Information Display*, Vol. 20, No. 8, 2012, pp. 413-440.
- [3] A. Holzinger, Finger Instead of Mouse: Touch Screens as a Means of Enhancing Universal Access, *LNCS*, Vol. 2615, 2003, pp. 387-397.
- [4] C. J. William and H. S. George, Discriminating Contact Sensor, *U.S. Patent 3911215A*, 1975.

- [5] G Barrett and R. Omote, Projected-Capacitive Touch Technology, *International Display Magazine*, Vol. 26, No. 3, 2010, pp. 16-21.
- [6] K. North and H. D'Souza, Acoustic Pulse Recognition Enters Touch-Screen Market, *Information Display*, Vol. 22, No. 12, 2006, pp. 22-25.
- [7] A. Butler, S. Izadi, and S. Hodges, Side Sight: Multi-Touch Interaction around Small Devices, in *21st Annual ACM Symposium User Interface Software Technology*, 2008, pp. 201-204.
- [8] G. Walker, Camera-Based Optical Touch Technology, *Information Display*, Vol. 26, No. 3, 2010, pp. 30-34.
- [9] A. Nathan and S. Gao, Interactive Displays: The Next Omnipresent Technology, *Proc. Of the IEEE*, Vol. 104, No. 8, 2016, pp. 1503-1507.
- [10] W. Grussenmeyer and E. Folmer, Accessible Touchscreen Technology for People with Visual Impairments: A Survey, *ACM Transactions on Accessible Computing*, Vol. 9, No. 2, 2017, Article 6 p31.
- [11] S. Chun and I.-S. Koo, Beam Projector Calibration System Based on Zigbee, *The Journal of the Institute of Internet, Broadcasting and Communication*, Vol. 11, No. 2, 2011, pp. 13-19.
- [12] S.-Y. Cho, Mathematical Methods to Locate Touch Points Using Laser Optic Modules, *International Journal of Circuits, Systems and Signal Processing*, Vol. 12, 2018, pp. 229-234.